PHYSICAL REVIEW B VOLUME 43, NUMBER 7 1 MARCH 1991

Magnetic properties of neodynium atoms in Nd-Fe multilayers studied by magnetic x-ray dichroism on Nd L_{II} and Fe K edges

F. Baudelet, E. Dartyge, and A. Fontaine
Laboratoire pour l'Utilisation du Rayonnement Electromagnétique, Université de Paris–Sud, 91405 Orsay, France

C. Brouder and G. Krill
Laboratoire de Physique des Solides, Université de Nancy I, Boîte Postale 239, 54506 Vandoeuvre-les-Nancy, France

J. P. Kappler
Institut de Physique et de Chimie des Matériaux de Strasbourg, Groupe d'Etude des Matériaux Métalliques, Université Louis Pasteur, 67070 Strasbourg, France

M. Piecuch
Laboratoire Mixte, Centre National de la Recherche Scientifique–Saint Gobain, Centre de Recherches de Pont-à-Mousson, Boîte Postale 109, 54704 Pont-à-Mousson, France

(Received 15 May 1990; revised manuscript received 8 August 1990)

In this paper we present an experimental investigation of the magnetic properties of metallic multilayers (here Nd-Fe) by magnetic x-ray dichroism (MXD). The magnetic absorption cross sections have been measured, using a dispersive optics, on both the L_{II} edge of Nd and the K edge of Fe in several Nd-Fe multilayers ($\Lambda \approx 40$–100 Å), for temperatures ranging from 77 to 300 K. We will show that the intensity of the magnetic absorption can be roughly correlated to the ordered magnetic moments present either on Nd or Fe, and thus the MXD allows direct information to be obtained on the local magnetic properties on a given atom. Moreover, by performing systematic studies as a function of the modulation length Λ, we discuss the efficiency of such experiments to yield *direct* information about the magnetic properties of the interfaces themselves. MXD experiments also give the sense of the coupling (ferromagnetic in the present case) between the magnetic moments of Nd and Fe in those systems. MXD results are compared to those given by bulk magnetization measurements and Mössbauer experiments on ^{57}Fe.

I. INTRODUCTION

Magnetic x-ray dichroism (MXD) is a high-energy spectroscopic method, which has recently been used both for the study of localized[1,2] and/or itinerant[3,4] magnetism in ordered magnetic systems. MXD is a very powerful tool for the study of the local magnetic properties, because it takes benefit both from the well-known selectivity of x-ray-absorption spectroscopy and from the polarization properties of synchrotron radiation. Here we present the first experimental investigation of the magnetic properties of a metallic multilayer by studying MXD with circular polarized synchrotron radiation (CPSR). In many aspects the polarization of light can be regarded as the "spin" of the photon (more precisely as its helicity). The extra angular momentum of the photon ($+h, -h, 0$ for left, right, or linear polarization) can be transferred to the atom (i.e., to the photoelectron) during the absorption process and, using the electric dipolar selection rules, it is possible to determine if the spin of the photoelectron is parallel or antiparallel to the "spin" of the photon. Thus, one can get access to the direction of magnetic moments.

Artificially modulated systems are now currently used in practical applications. This is particularly true for semiconductor-semiconductor superlattices and to a lesser extent for metal-nonmetal materials (e.g., for optical devices in the soft-x-ray range); for the case of metal-metal superlattices or multilayers it is true that the situation is less advanced but applications, particularly concerning the magnetic properties, will appear in the near future. It is well known that one of the keys to an understanding of the general properties of such modulated systems is to understand the structure and particularities of the interfaces. One of the most important conclusions we will try to extract from the experiments performed on these Nd-Fe multilayers is that MXD measurements are able to give valuable information about the magnetic properties of the interfaces themselves.

II. BASIC PRINCIPLES OF MAGNETIC X-RAY ABSORPTION IN CIRCULAR POLARIZED SYNCHTRON RADIATION

Dichroism simply reflects the fact that the absorption of an electromagnetic wave is polarization dependent. Dichroism can be either "natural" if due to structural properties (i.e., to symmetry, like chirality, for instance), or "magnetic" if the magnetic properties are involved. In this paper we shall focus on the last point. The best (and historical) example of magnetic dichroism is the well-known Faraday (or Kerr) effect, where the absorption coefficient (μ) in the optical range depends explicitly on the polarization of the electromagnetic wave:

$$\frac{\Delta\mu^{+-}}{\mu}=\frac{n''^{+}-n''^{-}}{n''^{+}+n''^{-}}$$

$(+,-)$ are associated with positive (left circular polarization) or negative helicity (right circular polarization), n'' is simply the imaginary part of the optical index $n=n'-in''$, which corresponds to absorption. It can be shown that $\Delta\mu^{+-}$ is proportional to the component of the nondiagonal conductivity tensor which depends explicitly on the magnetization of the sample and thus this dichroism is of magnetic origin. In our case, because we deal with high-energy photons [10 Å (1000 eV)$\rightarrow$1 Å (10 keV)], the processes involved in magnetic dichroism will be rather different from those which are at the origin of the Faraday (Kerr) effect. The interaction, in our case, can be simply described by the usual electrical dipolar Hamiltonian ($H_{\rm int}\alpha\varepsilon\cdot\mathbf{r}$) (we shall comment after on the possible contribution of electric quadrupolar interaction), whereas for the Faraday effect the dipolar magnetic term has to be taken into account. The fact that, at high photon energy, the interaction does not depend explicitly on the spin itself implies that the magnetic origin of the dichroism has been found indirectly (from the spin-orbit, for instance). For our purpose two rather different situations have to be considered: (i) either the photoelectron, according to the electrical dipolar selection rules, goes directly in highly localized states which are directly responsible for the existence of magnetic moments (e.g., $3d\rightarrow 4f$ transitions in the $M_{\rm IV,V}$ absorption edges of the rare-earth elements), (ii) or it enters some delocalized band which is not directly involved in building the magnetic moment (e.g., $1s\rightarrow 4p$ transitions in the K edge of Fe, or $2p\rightarrow 5d$ transitions in the $L_{\rm II,III}$ edges of rare-earth elements). In the first case the magnetic dichroism results from multiplet interactions and is rather well understood,[1,2] whereas in the second case, which corresponds to the situation encountered in this paper, it is really more difficult to describe. The similitude between both situations is that, at evidence, long-range order of the magnetic moments is needed, the major difference being that in situation (i) circular polarization of the light is not mandatory whereas it is absolutely needed in situation (ii).[3,4] Moreover if antiferromagnetic long-range order can contribute to "multiplet" MXD, only ferro(ferri)magnetic situations will be useful for the case we discuss in this paper.

From preliminary investigations,[4-6] it is rather simple to summarize what kind of conditions have to be fulfilled for the experimental observation of MXD.

The rate of circular polarization of the photon beam, defined as

$$P_{\rm ph}^{C}=\frac{n^{+}-n^{-}}{n^{+}+n^{-}}\ ,$$

where $n^{+}(n^{-})$ is the number of photons with left (right) polarization (i.e., a $\pm h$ "spin"), *must be nonzero.* If we assume no natural light in the beam, $P_{\rm ph}^{C}$ can be derived from the two measurements of the intensity of the linear polarized components:

$$|P_{\rm ph}^{C}|=\frac{2\sqrt{I_{\perp}I_{\parallel}}}{I_{\perp}+I_{\parallel}}\ .$$

There must be a difference between the spin-up and spin-down densities of unoccupied states for the final state of the photoelectron, i.e., $\rho_{\rm unoc}(\uparrow)\neq\rho_{\rm unoc}(\downarrow)$.

Here $\rho(\uparrow)$ $(\downarrow)$ are associated with majority (minority) spins.

Because of the spin independence of the Hamiltonian of the interaction, the absorption cross-section s is also spin independent. The spin dependence of the cross section comes out naturally from the spin-orbit interaction either in the initial or in *the final state* and is related to the Fano effect[7] (see the discussion below).

Considering the symmetry of the problem, it is quite clear that the direction of the magnetization and the helicity of the photons play the same role. The effect depends only on the relative direction of these two quantities and thus, what we need is to measure independently the absorption cross section (σ) for two situations.

(a) Either the helicity of the photons and the magnetization are parallel. (b) Either the helicity of the photons and the magnetization are antiparallel.

In our study, the polarization of the photons is mainly right ($-h$) (see Sec. III) and *is kept constant during the experiment,* the direction of the magnetization is changed by applying a magnetic field (≈ 1 T) either parallel or antiparallel to the direction of propagation of the photons ($\mathbf{k}$). We suppose in a first step that there is no magnetic anisotropy.

To analyze experimental spectra, it is important to specify precisely all our conventions. We take the x-ray wave vector as our z axis. We define up (down) spins as spins parallel (antiparallel) to the z axis, respectively. To make a connection between experimental spectra and the spin polarization of photoabsorbing atoms, we use the basic ingredients of the electronic structure theory of itinerant magnetism. For a $L_{\rm II,III}$ edge we consider that the final states can be written as a product of a space wave function by a spin state (e.g., $|f^{\uparrow}\rangle=f(\mathbf{r})|\uparrow\rangle$). This is an approximation relevant for itinerant magnetism, which is valid in describing the spin polarization of the final d states of the photoelectron. It neglects spin-orbit coupling in the final state.

Then the absorption cross section can be written[8]

$$\sigma(\hat{\varepsilon})=4\pi^{2}\alpha\,\mathrm{tr}\omega\sum_{f,m_j}\left(|\langle f^{\uparrow}|\hat{\varepsilon}\cdot\mathbf{r}|jm_j\rangle|^{2}+|\langle f^{\downarrow}|\hat{\varepsilon}\cdot\mathbf{r}|jm_j\rangle|^{2}\right).$$

The initial states can be expanded over spin states and spherical harmonics, using Clebsch-Gordan coefficients:

$$|jm_j\rangle = \sum_{m,s} (lm\tfrac{1}{2}s|jm_j)\phi_{lj}(r)Y_l^m(\hat{\mathbf{r}})|s\rangle ,$$

where $\phi_{lj}(r)$ is the radial core hole wave function. The absorption coefficient of left (+) and right (−) circularly polarized x rays are then obtained by noticing that

$$\hat{\boldsymbol{\varepsilon}}^{+}\cdot\mathbf{r} = -\left(\frac{4\pi}{3}\right)^{1/2} rY_1^1(\hat{r}) ,$$

$$\hat{\boldsymbol{\varepsilon}}^{-}\cdot\mathbf{r} = \left(\frac{4\pi}{3}\right)^{1/2} rY_1^{-1}(\hat{r}) .$$

Then, neglecting the effect of the final states with s symmetry, it can be shown that for an L_{II} edge:[8]

$$\sigma^{+} = \sigma^{\uparrow}_{2\,1/2} + 3\sigma^{\downarrow}_{2\,1/2}, \quad \sigma^{-} = 3\sigma^{\uparrow}_{2\,1/2} + \sigma^{\downarrow}_{2\,1/2} ,$$

while for an L_{III} edge,

$$\sigma^{+} = 5\sigma^{\uparrow}_{2\,3/2} + 3\sigma^{\downarrow}_{2\,3/2} \quad \sigma^{-} = 3\sigma^{\uparrow}_{2\,3/2} + 5\sigma^{\downarrow}_{2\,3/2}$$

where σ^{s}_{2j} is a reduced transition probability from the "state" $\phi_{lj}(r)$ to the d component of the final states with spin s. These formulas show that the transition produced by right-polarized x rays are preferentially toward spin-up states at an L_{II} edge, and spin-down states at an L_{III} edge. The reverse is true to left-polarized x rays. The above expressions were obtained by Erskine and Stern[9] in the case of nickel. It is shown in Ref. 8 that they are valid for any crystallographic structure when the sample is a powder. It is possible to relate the reduced transition probabilities σ^{s}_{2j} to the density of d states with spin-polarization s obtained within the band-structure formalism.[3–5,10]

Let us consider how this can be used to find the spin polarization of the d states of the photoabsorbing species. At LURE we use right-polarized x rays (σ^{-}), and we switch the magnetic field direction. Let $\sigma^{-}(B)$ [$\sigma^{-}(-B)$] be the spectrum observed with the magnetic field applied parallel (antiparallel) to the z axis. We assume that the sample is ferro- or ferrimagnetic and saturated, so that the electronic spins are either parallel or antiparallel to the z axis. Let $\sigma^{\uparrow}2j$ be the reduced transition probability toward up spins when the field is $+B$. Inverting the magnetic field reverses all the spin states so that the reduced transition probability toward down spins with field ($-B$) is the reduced transition probability toward up spins with field ($+B$). We plot the quantity Δ defined by

$$\Delta = \frac{\sigma^{-}(B)-\sigma^{-}(-B)}{\sigma^{-}(B)+\sigma^{-}(-B)} = \frac{3\sigma^{\uparrow}_{2\,1/2}+\sigma^{\downarrow}_{2\,1/2}-\sigma^{\uparrow}_{2\,1/2}-3\sigma^{\downarrow}_{2\,1/2}}{3\sigma^{\uparrow}_{2\,1/2}+\sigma^{\downarrow}_{2\,1/2}+\sigma^{\uparrow}_{2\,1/2}+3\sigma^{\downarrow}_{2\,1/2}} = \frac{\sigma^{\uparrow}_{2\,1/2}-\sigma^{\downarrow}_{2\,1/2}}{2(\sigma^{\uparrow}_{2\,1/2}+\sigma^{\downarrow}_{2\,1/2})}$$

taking the example of an L_{II} edge. Therefore, if $\Delta > 0$, we have a majority of up spins when the field is parallel to the x-ray beam direction, if $\Delta < 0$, a majority of spins are down when the field is parallel to the x-ray beam direction. The inverse relation holds at an L_{III} edge.

If the x-ray is not fully polarized, the observed effect is at an L_{II} edge

$$\Delta = -P^{C}_{\mathrm{ph}}\frac{\sigma^{\uparrow}_{2\,1/2}-\sigma^{\downarrow}_{2\,1/2}}{2(\sigma^{\uparrow}_{2\,1/2}+\sigma^{\downarrow}_{2\,1/2})} ,$$

while at an L_{III} edge

$$\Delta = P^{C}_{\mathrm{ph}}\frac{\sigma^{\uparrow}_{2\,3/2}-\sigma^{\downarrow}_{2\,3/2}}{(\sigma^{\uparrow}_{2\,3/2}+\sigma^{\downarrow}_{2\,3/2})} .$$

Notice that, if the radial core hole wave functions $\phi_{lj}(r)$ are not too much different for $j=\frac{1}{2}$ (L_{II} edge) and $j=\frac{3}{2}$ (L_{III} edge), then we obtain the relation $\Delta(L_{\mathrm{II}}) = -2\Delta(L_{\mathrm{III}})$, which is often observed experimentally.

For the K edge, the situation is much more delicate since MXD is due to spin-orbit coupling in the final state (there is none in the initial state). A detailed analysis of MXD at the K edge[8] shows that the dichroic effect is due mainly to spin-orbit coupling of the photoelectron on the absorbing site. But it is not directly related to the spin density of p states. Moreover, the weights of $\sigma^{\uparrow}_{1\,1/2}$ and $\sigma^{\downarrow}_{1\,1/2}$ are not as simple as for L_{II} or L_{III} edges: they depend on energy and they can even change sign. They decrease rapidly with photoelectron energy, and this explains why no spin-polarized EXAFS was observed at the K edge. Therefore, it is more difficult to find the spin polarization of the final states from experimental K-edge MXD spectra. However, useful information can be gained by comparison with reference spectra.

In summary, from MXD in CPSR, it is possible in principle to get information about the spin polarization of the empty states in ordered systems and thus, because these empty states are polarized by all the other electrons, to evidence magnetic effects. For instance, K-edge experiments on Fe (Ref. 3) probe the spin polarization of empty $4p$ states which are polarized by the $3d$ electrons.[10] At evidence the appearing feature is that this probe is *local and selective*. The other obvious advantage is that the coupling between the magnetic moments can be determined and we will give an example of such a possibility in this study of Nd-Fe multilayers.

III. EXPERIMENTAL SET-UP FOR MXD EXPERIMENTS USING A DISPERSIVE OPTICS

A. General aspects of dispersive x-ray absorption spectroscopy

The energy dispersive optics based spectrometer allows us to collect XAS data in transmission mode exclusively. It is merely a combination of a dispersive geometry with a position-sensitive detector able to work under high-flux conditions. It permits *in situ* and time-resolved investigations. The recent development of measurements of magnetic x-ray dichroism takes advantage of specific characteristics of this experimental scheme (Fig. 1). The optics,

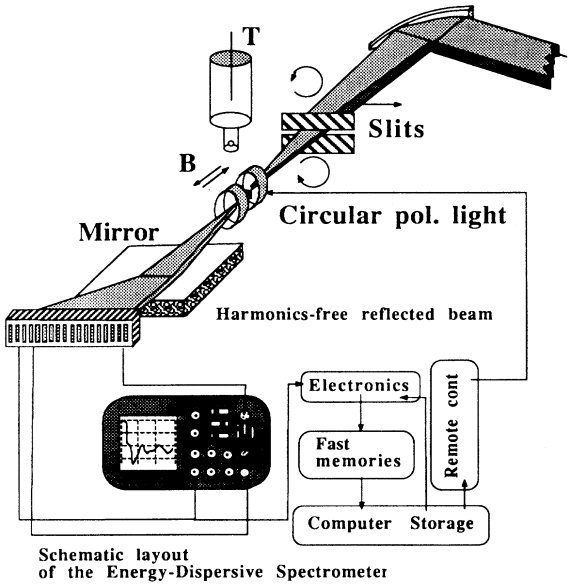

FIG. 1. Experimental set-up used for dispersive MXD at LURE.

which consists of a 23-cm-long bent silicon crystal, reflect in the horizontal plane and a flat mirror rejects harmonics. The Si crystal is shaped elliptically to match the bending magnet source and the sample position at the two-focus. This optics acts as a wide bandpass energy filter since the incident angle varies continuously along the crystal. The energy direction correlation is converted into an energy position correlation on a photodiode array made of 1024 pixels. 6×10^4 photons per pixel (6×10^8 for 1024 pixels) can be read every 2.5 msec with a statistics-limited signal-to-noise ratio of 250 and directly digitized by a fast 10-bit-CAD and stored into a computer to build an XAS signal. Improvement of the signal-to-noise ratio of each data point (larger than 1000 in terms of accuracy of the absorption) is currently achieved by accumulation of 32 frames.

B. Advantages of dispersive optics for MXD

Fox MXD measurements, the energy dispersive spectrometer shows intrinsic advantages and one usual limitation.

(a) The bent crystal reflects within the horizontal plane and therefore do not attenuate the vertical component of the electric field of the light. This is favorable to keep high flux with circular polarization since it is the minor component which is undamped. This point is an obvious advantage over the two-crystal set-up for which keeping a constant tuning between the two crystals is a real challenge. On the contrary, the transfer of circular polarization by the optics with a single reflection leads to a very stable circular-polarization rate which can be considered constant over the energy range. This is more questionable with the two-crystal monochromator, especially when the Bragg angle approaches 45°. The Darwin width of the vertical component includes the $\cos2\theta$ term and hence is is not very easy to keep the narrow profile of the second crystal from exactly overlapping the first one through the whole scan. The lack of mechanical movement of the dispersive scheme keeps the polarization rate constant during the whole experiment.

(b) An extreme sensitivity to small differences in intensity, typically of 10^{-3} can be achieved without adding more than 32 frames, since there is no vibration-induced noise and a rigorous energy-scale stability. For this last point, the limitation comes from a temperature change of the crystal due to the beam decay: (2.0° within 2 h) which keeps the energy shift smaller than 30 meV at 7 keV with Si(311) as a Bragg reflector.

(c) The small size of the polychromatic focus allows us to work with a small sample (≈1 mm) and therefore a "high" magnetic field can be obtained (up to 1.3 T in our experimental set-up).

(d) The dispersive optics allows only data collection in the transmission mode. It is therefore impossible to access to fluorescence detection, which is a very appealing scheme to measure thin films (even monolayers deposited on a surface).

C. Selection of the beam

The first step in our experiments is to select the beam part with a sufficient rate of right (or left) circularly polarized light, i.e., to slit the beam in the low (or high) side of the vertical intensity distribution. We work at an inclined angle of view (0.4 mrad) below the orbit plane of the positrons stored in DCI at LURE which gives a polarization rate (≈0.9) after the polychromator. In this operation, we "loose" 90% of the beam intensity compared to the intensity available at the center of the vertical distribution. The possibility to record the vertical profile using the photodiode array put vertically allows us to visualize the selection of the beam. Horizontal slits installed after the polychromator are positioned with a precision of the pixel size (25 μ). The full illumination of the Bragg crystal avoids large thermal gradients which damage the crystal.

We evaluated the circular polarization rate of the beam $P^c_{\rm ph}$ by measuring the linear polarization rate $P^L_{\rm ph}$ and assuming that $P^{2L}_{\rm ph}+P^{2c}_{\rm ph}=1$. The linear rate of polarization was measured at the sample position (behind the Si polychromator) by recording the intensity scattered by a kapton foil along the horizontal and vertical directions at an angle $2\theta=90°$.

D. Data collection

Since data are collected with an accurate periodicity, a computer-controlled magnetic-field inversion improves the signal-to-noise ratio. Typically, 180 successive spectra made of 32 frames are usually collected. In that way, we can cancel almost exactly, the derivativelike signal due to the thermal shift of the Si crystal, which can be a significant part of the real MXD signal. With a minor mathematical treatment of this periodic-data acquisition

TABLE I. Magnetic moments deduced from magnetization measurements ($T=4$ K and $H=2$ T) and Mössbauer experiments (see text).

Sample	$\mu(\mu_B/\text{f.u.})$	$\mu_{Fe}(\mu_B/\text{atom})$	$\mu_{Nd}(\mu_B/\text{atom})$
Nd_{35}-Fe_{15}	1.92	1.75	2.1±0.1
Nd_{35}-Fe_{30}	2.35	2.1	2.9±0.1
Nd_{20}-Fe_{35}	2.60	2.1	3.1±0.1
Nd_{45}-Fe_{35}	2.20	2.1	2.5±0.1
Nd_{60}-Fe_{35}	1.60	2.1	1.4±0.1

we are able to eliminate accurately the thermal part of the differential signal and yield a signal-to-noise (difference signal-to-noise) ratio of 20 after 240 acquisitions, i.e., 7680 spectra (240×32), in 9 h at the Fe K edge using Si(311). With a small loss of energy resolution the Si(111) optics reduces by a factor 10 typically the data collection time.

E. Experimental conditions

The MXD experiments have been performed, in a magnetic field up to 1.3 T and in the temperature range from 80 to 300 K, at the Fe K edge (7112 eV) and the Nd L_{II} edge (6722 eV), using a curvature radius of the Si(311) polychromator, yielding a 150-eV energy band above the edge. This last value can be increased by a factor of 2 by simply increasing the crystal curvature or changing to the 111 Miller indexes. It is thus possible to get a spin-dependent EXAFS signal to 200 eV above the edges.

A liquid-He-cooled cryostat is now installed allowing measurements down to 4 K.

IV. MAGNETIC AND STRUCTURAL PROPERTIES OF ND-FE MULTILAYERS

Nd-Fe multilayers have been prepared in a wide range of modulation lengths (Λ:40–100 Å), by evaporation of Nd and Fe under ultrahigh vacuum conditions.[11] The magnetic properties have been determined by bulk magnetization measurements between 4 and 300 K and into magnetic field up to 20 T.[12] The magnetic moment on Fe atoms has been derived (in a few cases) by Mössbauer spectroscopy on ^{57}Fe assuming a linear relation between the magnetic moment and the hyperfine field: $\mu(\mu_B/\text{atom})=H_{hyp}$ (kOe)/145.

From these magnetic measurements, it is possible to deduce four fundamental truths.

(1) The magnetic moment on both the iron and the neodymium atoms at 4 K and $H=2$ T (Table I).

(2) The sign of the coupling between the Nd and Fe moments which appears to be ferromagnetic.

(3) The easy axis of magnetization which, in the case we discuss in this paper, is perpendicular to the film planes at 4 K and in the planes at 300 K. Even in this last situation, for a 1-T magnetic field, it appears that the magnetization is parallel to the field indicating that the magnetic anisotropy has been overcome.

(4) From the quantitative analysis of the Mössbauer spectra, it is possible to estimate the width of the interface between Nd and Fe (e_i) which is roughly 8 Å. This

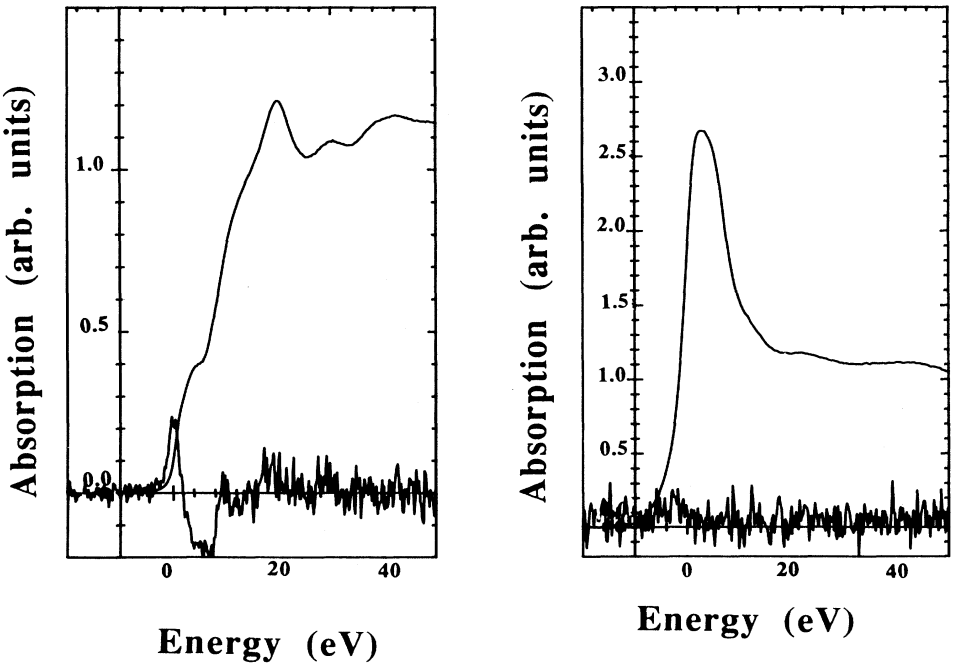

FIG. 2. Magnetic x-ray absorption compared with the absorption cross section observed at 300 K and 1 T on the K edge of iron metal (left curve) and the L_{II} edge of neodymium metal (right curve). The magnetic signal is multiplied by a factor of 200 for both spectra.

means that each interface is made from two to three layers of interdiffused Nd-Fe alloys.

V. MXD RESULTS ON THE ND-FE MULTILAYERS SYSTEM

First let us show in Fig. 2, the results we obtained at $T=300$ K in the case of pure bcc Fe (K edge) (1 h of data acquisition) and dhcp Nd (L_{II} edge) 10′ data acquisition). We notice the existence of a MXD signal on Fe (in good agreement with the earlier results of Schütz *et al.*[3]) and its absence for pure Nd. These results agree with the fact that Fe is ferromagnetic and Nd is paramagnetic at room temperature. According to the discussion of Sec. II, the sign of the MXD signal is related with the orientation of the photoelectron spin ($4p$ in the case of Fe K edge) and we have underlined the difficulties which can be encountered in the case of K-edge studies. In the following, we assume that the sign of the MXD at the K edge of iron gives us directly the spin polarization of the $3d$ bands in iron. This assumption is supported by the analysis of many experimental spectra.

In Fig. 3 we report similar results obtained on a rhombohedral Nd_2Fe_{17} compound which is ferromagnetic at room temperature. The Curie temperature is $T_c \approx 350$ K (Ref. 13) and the magnetic moments on Nd($\approx 1.3\ \mu_B$/atom) and Fe($\approx 2.2\ \mu_B$/atom) are coupled ferromagnetically. We notice the "strong" MXD signal detected at the Nd L_{II} edge which is $\approx 10\%$ of the total absorption cross section. Here we must underline the fact that the strength of this effect reflects the polarization of the $5d$ orbitals of Nd by the $3d$ electrons of Fe (in the Nd_2Fe_{17} structure the Nd atoms are surrounded by Fe atoms). Similar effects have been observed on other compounds, like $GdFe_2$, for instance Ref. 14, where the MXD signal on Gd is stronger than that observed for pure Gd metal. The sign of the MXD signals we observed in Nd_2Fe_{17} confirms that the $3d$ spins are antiparallel to the Nd $4f$ spins, assuming that here the $5d$ and $4f$ spins are parallel. Thus, because we are at the beginning of the lanthanide series (i.e., $J=L-S$), the net coupling between the magnetic moment of Nd and Fe is ferromagnetic. The general shape of the Nd L_{II} and MXD signals in Nd_2Fe_{17} allows us to briefly address the possible role of electrical quadrupolar transitions to the MXD effect. Indeed, such transitions imply a change in the $4f$ occupancy in the final state, simply because of the selection rules ($\Delta l=\pm 2$), thus those contributions should arise at the very beginning of the edge (≈ 8 eV) below the main $5d$ contribution of dipolar origin). We notice in Fig. 2, that no significant signal is present in this energy range (a detailed calculation for Gd, Carra and Altarelli,[15] shows that quadrupole contribution may be as large as 15% of the main peak), thus we can safely conclude that for our present study quadrupole effects may be neglected.

Let us now present the results obtained on the Nd-Fe multilayers. Two series of experiments have been performed between 80 and 300 K in a 1-T magnetic field: the first has been made on multilayers where the Nd thickness was kept constant ($e_{Nd} \approx 35$ Å) and the Fe thickness was increased from 15 to 35 Å, the second one being made for a constant Fe thickness ($e_{Fe} \approx 35$ Å) and a variable Nd one (20 Å → 60 Å).

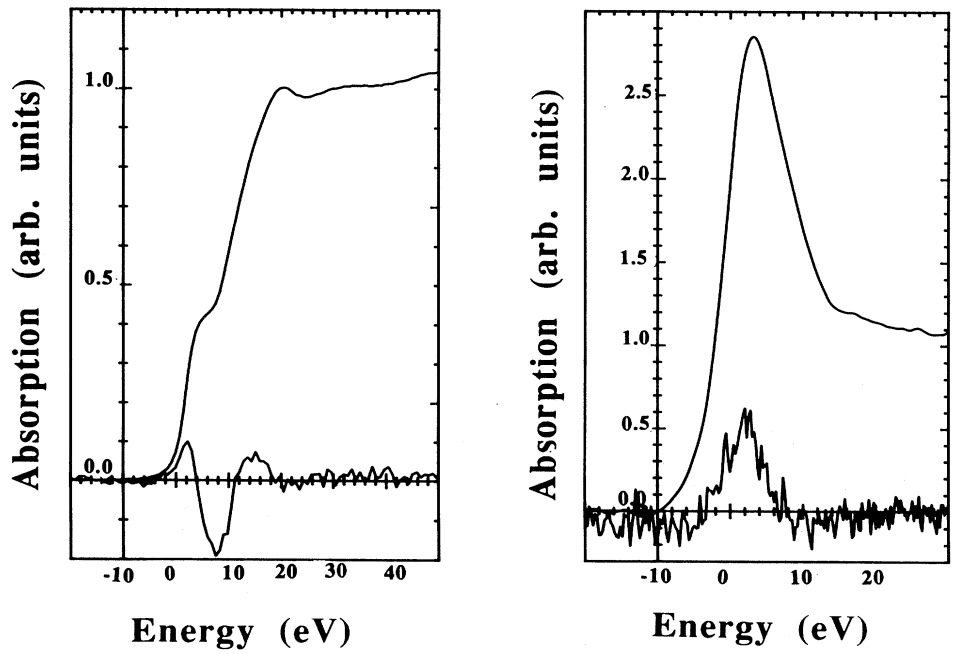

FIG. 3. Same as Fig. 2 for Nd_2Fe_{17}; left: Fe K edge, magnetic signal multiplied by a factor of 200; right: Nd L_{II} edge, magnetic signal multiplied by a factor of 20.

A. Results at 300 K (origin of the MXD signal on Nd atoms)

The MXD signal of Fe is rather insensitive both to the thickness and temperature parameters except for the case of very low Fe thickness ($e \leq 15$ Å). Thus we show in Fig. 4 the signal observed on Nd_{20}-Fe_{35} (20 Å of Nd and 35 Å of Fe) which can be considered as typical of the situation on Fe that we will consider in this paper. The similitude between the situation of pure bcc Fe is clearly evident. The situation is obviously different in the case of Nd. In Figs. 5(a) and 5(b) we report the MXD signals recorded at the Nd L_{II} edges. Let us mention that we checked that these signals were independent of the angle between the magnetic field and normal to the layer's plane, and thus we can conclude that magnetic anisotropy does not play any significant role in a 1-T magnetic field. The dependence of the overall intensity of the MXD signal shows clearly that it originates from the iron atoms themselves: its strength is proportional to the iron thickness and inversely proportional to the neodymium thickness. These results show that *even* at room temperature at least some of the *Nd magnetic moments* couple ferromagnetically with the iron moments (this is given by the sign of the MXD, the situation is similar to that observed for Nd_2Fe_{17}).

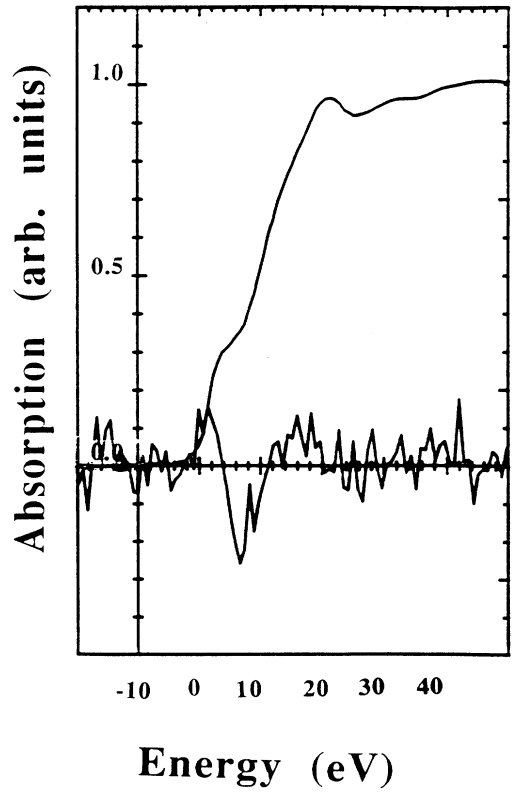

FIG. 4. Magnetic x-ray absorption at $T=300$ K on the Fe K edge of a $Nd_{20\,Å}$-$Fe_{35\,Å}$ multilayer. Magnetic signal multiplied by a factor of 100.

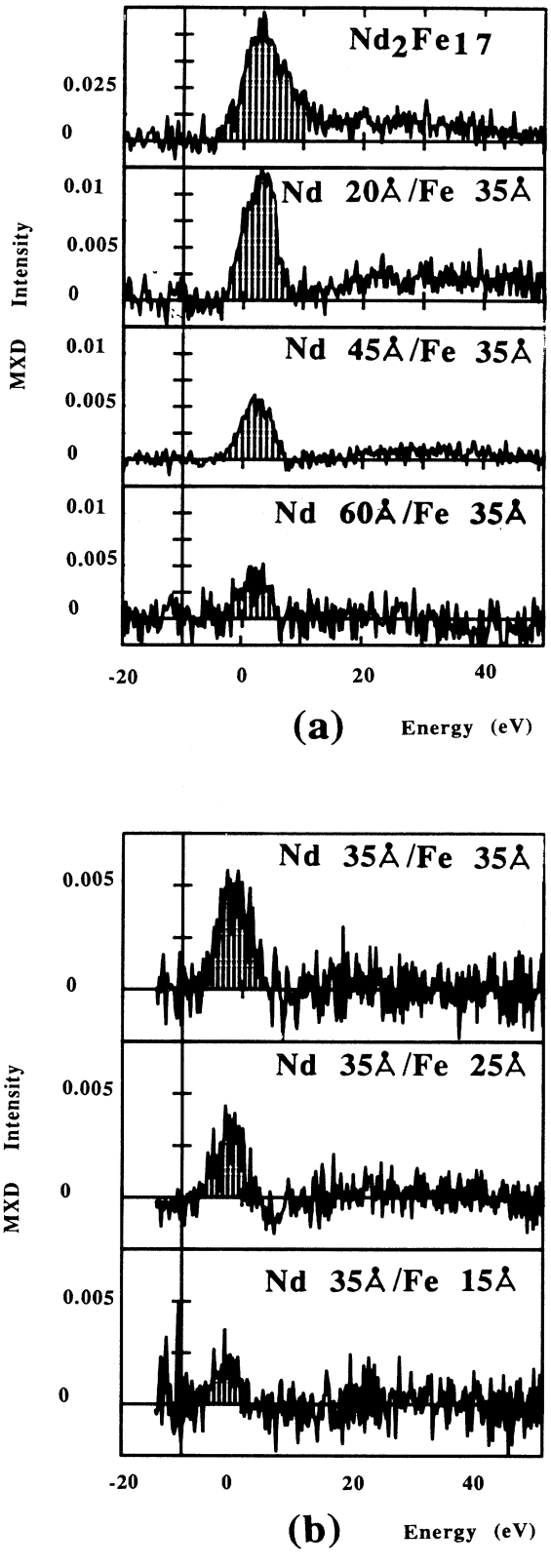

FIG. 5. Magnetic x-ray absorption at $T=300$ K observed on the Nd L_{II} edges; (a) as a function of the Nd thickness; (b) as a function of the Fe thickness.

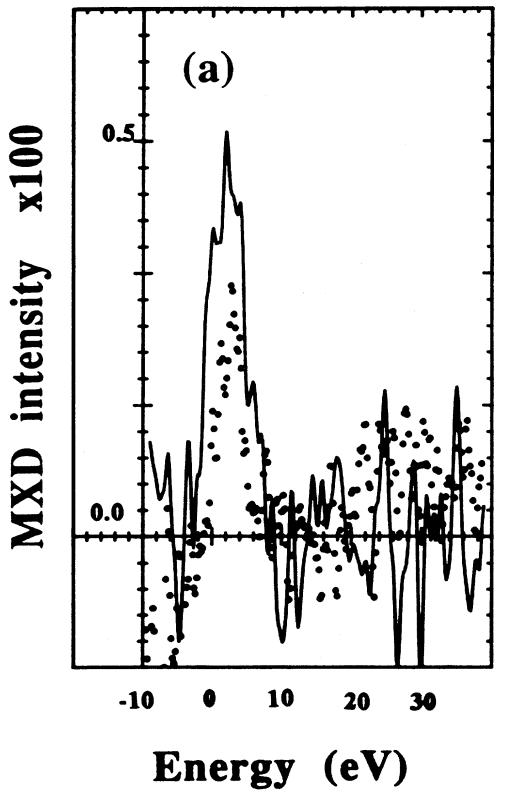

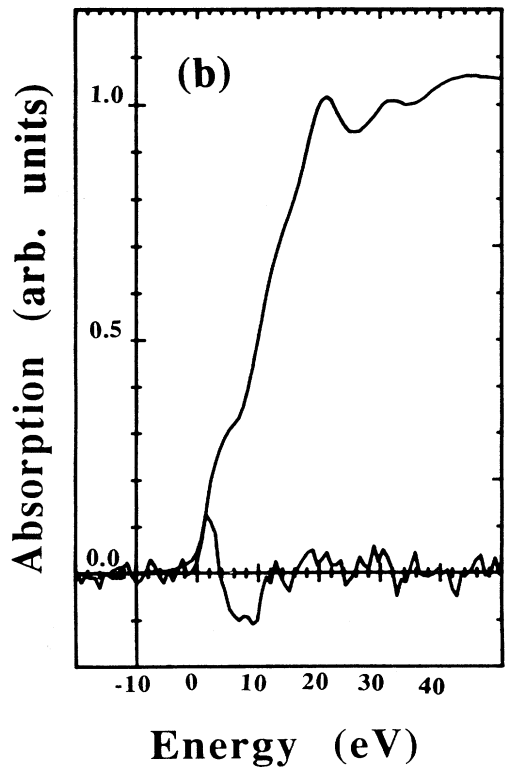

FIG. 6. Magnetic x-ray absorption; (a) at $T=300$ K for the $Nd_{35\,Å}$-$Fe_{35\,Å}$ multilayer on the Nd L_{II} edge before and after {dashed curve} diffusion; (b) on the Fe K edge after diffusion. The magnetic signals are multiplied by a factor of 200.

The question is obviously to understand where these atoms are located and, more important, in what kind of local environment they are imbedded. The dependence of the MXD signal on the Nd thickness shows clearly that the magnetic Nd ions are preferentially located near the interface but it is difficult to deduce any valuable conclusions concerning the local environment of these magnetic Nd atoms. Clearly speaking, we do not know if these atoms are those involved in the formation of the Nd-Fe alloys at the interface (see Sec. IV) or if other Nd atoms may be concerned (i.e., more far away from the interface). We shall see that more conclusive statements can be made from low-temperature measurements.

A preliminary, but not absolutely conclusive, indication can be obtained if we consider what happens to the XMD signal if we induce the diffusion between Nd and Fe by heating the sample at 500 K for 6 h. This is shown in Fig. 6 for the Nd_{35}-Fe_{35} sample where we notice the strong decrease of the Nd MXD signal after diffusion. However, this result is ambiguous because it can be explained in two opposite ways: either it is an indication that Nd-Fe alloys at the interface play the minor role (simply because the interface is more diffuse and that experimentally we notice the decrease of the MXD contribution), or it reflects both the progressive enrichment in Nd of the Nd-Fe alloys at the interface (which become nonmagnetic) and the reduction of the thickness of bcc Fe.

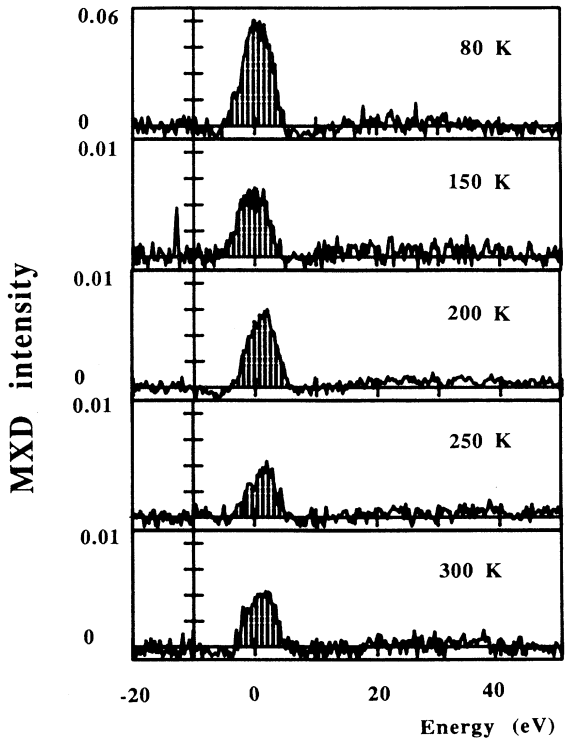

FIG. 7. Temperature behavior of the magnetic x-ray absorption on the Nd L_{II} edge in the $Nd_{20\,Å}$-$Fe_{35\,Å}$ multilayer.

B. Behavior of MXD on Nd with temperature (comparison with magnetization results)

In Fig. 7 we report the typical behavior with temperature of the MXD signal on Nd in Nd-Fe multilayers (here the case $Nd_{20}Fe_{35}$ is shown). The integrated intensity of the MXD signal can be correlated to the value of the ordered magnetic moment on Nd and thus can be compared to the values we extract from the magnetization measurements. This is done in Fig. 8 for several Nd_xFe_{35} samples. The normalization has been made for the sample $Nd_{20\,Å}$-$Fe_{35\,Å}$ at $T=100$ K, where it is found that the magnetic moment is near its maximum value corresponding to $J_z=\frac{9}{2}$ ($gJ_z=3.27\ \mu_B$/atom). We see that the agreement is not too bad between both sets of data. The observed discrepancies for the larger Nd thickness may be correlated to the fact that the magnetic moments on Nd have been deduced by assuming that the magnetic moments on Fe are constant and independent of the Nd thickness (see Sec. IV). Thus, we should not worry, in a first step, about such disagreements. In Fig. 9(a), the behavior of the magnetic moments on Nd, at $T=4$ K (deduced from magnetization measurements), with the inverse of the Nd thickness (e^{-1}) is reported. It can be compared with similar variation of the integrated intensity of the MXD signal [Fig. 9(b)]. The most obvious way to understand these results is to interpret the parameter $e_M \approx 30$ Å (see Fig. 9) which corresponds to the Nd thickness where the full magnetic moment of Nd should be obtained, as the effective magnetic thickness of Nd layers in the case of $Nd_{x\,Å}$-$Fe_{35\,Å}$ samples. As mentioned in Sec. IV, the Mössbauer experiments yield an upper limit of 8 Å for the interface thickness (e_I) between Nd and Fe, thus e_M is definitely larger than e_I [obviously in the case of ultrathin Fe layers (≈ 15 Å) the distinction between e_I and e_M becomes doubtful but it is meaningful for thicker Fe layers. We must keep in mind that an 8-Å interface is built by only two iron layers (i.e., $\approx$4–5 Å), this has been confirmed both from Mössbauer[11,12] and recent anomalous small angle x-ray scattering experiments[16]]. Such results imply that the exchange interaction between the electrons is sufficient to induce the ordering of the magnetic moments on Nd on a range of ≈ 15 Å on each side of the interface. Therefore the Nd atoms which are concerned by these "long"-range exchange interactions are not only those embedded in the interface.

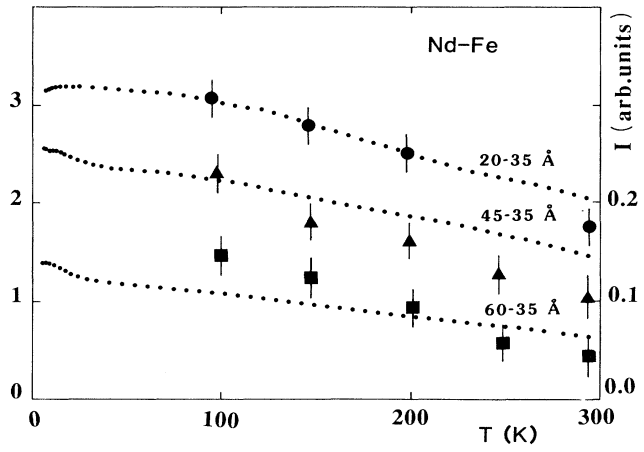

FIG. 8. Comparison between the Nd L_{II} MXD and the magnetization results. Dotted lines: magnetic measurements.

VI. CONCLUSION

This study has to be considered as a prospective for the use of MXD in general problems involving magnetism, including the special case of artificial modulated structures (superlattices, multilayers, thin films, etc,. . .) where specific problems concerning the magnetism of the interfaces can be addressed. This technique could give valuable information and should be complementary to other measurements, such as magnetic x-ray diffraction,[17]

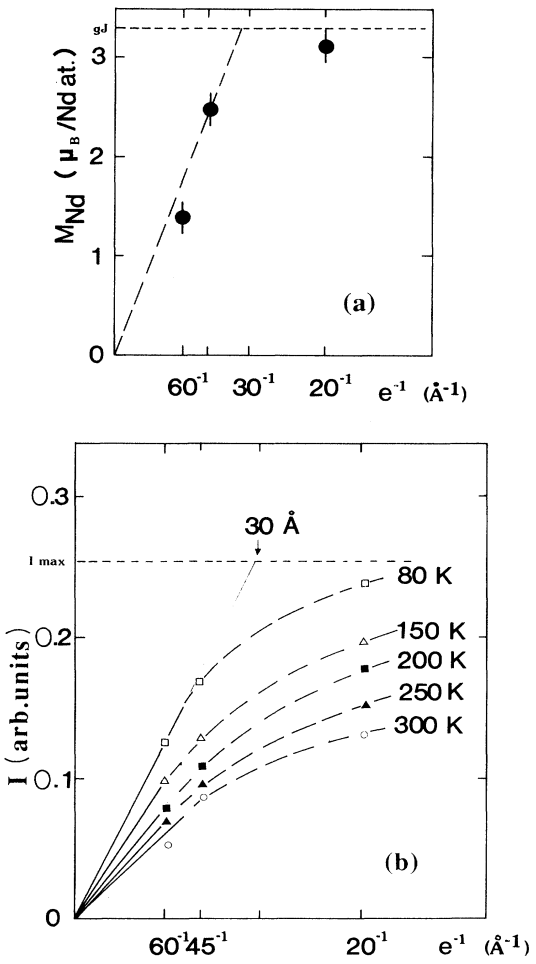

FIG. 9. (a) Behavior of the magnetic moment of Nd (at $T=4$ K and $H=2$ T) with the inverse Nd thickness. (b) Behavior of the Nd MXD with the inverse Nd thickness.

neutrons scattering, etc. The obvious advantage of MXD is that it gives direct information on the magnetic properties of the atom which is probed by the photon. With the recent developments of new and intense sources delivering high flux of circularly polarized photons,[18] we believe that MXD will be a unique tool for the determination of local magnetic properties of atoms in condensed matter.

ACKNOWLEDGMENTS

The Laboratoire pour l'Utilisation du Rayonnement Electromagnétique, the Laboratoire de Physique des Solides, IPCMS, G.E.M.M.E., and Laboratoire Mixte are Unités Associées au Centre National de la Recherche Scientifique Nos. 8, 155, 380046, and 37, respectively.

[1]B. T. Thole, G. van der Laan, and G. Sawatzky, Phy. Rev. Lett. **55**, 2086 (1985).

[2]G. van der Laan, B. T. Thole, G. Sawatzky, J. B. Goedkoop, J. C. Fuggle, J. M. Esteva, R. Karnatak, J. P. Remeika, and H. A. Dabkowska, Phys. Rev. B **34**, 6529 (1986).

[3]G. Schütz, W. Wagner, W. Wilhem, P. Kienle, R. Zeller, R. Frahm, and G. Materlik, Phys. Rev. Lett. **58**, 737 (1987).

[4]G. Schütz, M. Knülle, W. Wagner, W. Wilhem, P. Kienle, R. Zeller, and R. Frahm, Z. Phys. B **73**, 67 (1988).

[5]G. Schütz and R. Wienke, Hyperfine Inter. **50**, 457 (1989).

[6]C. Brouder, D. Malterre and G. Krill, in *Absorption X Magnétique,* proceedings of the Spring School, Rayonnement Synchrotron Polarisé circulairement, Electrons polarisés et Magnétisme, Mittelwihr 1989, edited by E. Beaurepaire (CNRS, Strasbourg, 1989), p. 115.

[7]U. Fano, Phys. Rev. B **178**, 131 (1969).

[8]C. Brouder and M. Hikam, Phys. Rev. B **43**, 3809 (1991).

[9]J. L. Erskine and E. A. Stern, Phys. Rev. B **12**, 5016 (1975).

[10]H. Ebert, P. Strange, and B. L. Gyorffy, Z. Phys. B **73**, 77 (1988).

[11]M. Piecuch, L. T. Baczewski, J. Durand, G. Marchal, P. Delcroix, and H. Nabli, J. Phys. (Paris) **C8-12**, 1755 (1988).

[12]L. T. Baczewski, M. Piecuch, J. Durand, G. Marchal, and P. Delcroix, Phys. Rev. B **40**, 11237 (1989).

[13]H. R. Kirchmayr and C. A. Poldy. J. Magn. Magn. Mater. **8**, 1 (1978).

[14]F. Baudelet, E. Dartyge, G. Krill, J. P. Kappler, C. Brouder, M. Piecuch, and A. Fontaine (unpublished).

[15]P. Carra and M. Altarelli, Phys. Rev. Lett. **64**, 11 (1990); **64**, 1286 (1990).

[16]J. P. Simon, O. Lyon, A. Bruson, M. Piecuch, and F. Rieutord, in *Proceedings of the Second International Conference, Progress in X-ray Studies by Synchrotron Radiation,* Rome, 1989, edited by A. Balerna (Italian Physical Society, Rome, 1989), p. 789.

[17]D. Gibbs, D. R. Harshman, E. D. Isaacs, D. B. McWhan, D. Mills, and C. Vettier, Phys. Rev. Lett. **61**, 1241 (1988).

[18]J. Goulon, P. Elleaume, and D. Raoux, Nucl. Instrum. Methods **A254**, 192 (1987).